Asian Journal of Agriculture and Rural Development
Volume 15, Issue 2 (2025): 281-290

Soil EC index – based prediction of rice growing and yield in the Mekong Delta

The Anh Ho[a,b]
Van Khanh Nguyen[a]
Van Huu Bui[a]
Chi Ngon Nguyen[a]

[a]*College of Engineering, Can Tho University, Vietnam.*
[b]*Faculty of Mechanical Engineering, Can Tho University of Technology, Vietnam.*

ncngon@ctu.edu.vn (Corresponding author)

Article History
Received: 17 April 2025
Revised: 2 June 2025
Accepted: 13 June 2025
Published: 18 June 2025

Keywords
Soil electrical conductivity
Mekong Delta
LSTM model
NDRE
NDVI
Rice yields.

ABSTRACT
This research explores the use of soil electrical conductivity (EC) in rice cultivation, focusing on soil EC correlation with vegetation indices (NDVI, NDRE) and soil EC impact on yield. A total of 228 soil EC, NDVI, and NDRE data points were collected from an 11,000 m² field in Hau Giang and Can Tho City. Soil EC was measured at the beginning of the season, and at 39 and 49 days after sowing. NDVI was recorded on days 39, 49, 60, and 72, with initial values set to zero due to no crop presence. Results show that soil EC decreased from the start to day 49, while NDVI and NDRE increased. Spearman correlation analysis revealed strong relationships between early soil EC and NDVI at days 39 and 49 (r = 0.82, 0.71), and between soil EC at day 49 (EC 49) and NDRE at later stages (r = 0.594, 0.565). Additionally, 150 soil EC and yield samples from five Mekong Delta regions were used in an LSTM model (70% training, 30% testing), achieving high accuracy (RMSE = 0.0919, MAE = 0.0634, R^2 = 0.8492). The findings suggest that soil EC is a valuable indicator for monitoring crop growth and managing rice production, particularly in areas affected by salinity due to climate change.

Contribution/Originality: This study measured soil EC in the Mekong Delta, Vietnam, where effective field measurement tools are scarce. It explores soil EC's application in managing crop growth (assessed via NDVI). The LSTM model, combined with soil EC data, effectively predicts rice yield, enabling the selection of optimal cultivation areas under climate change conditions.

DOI: 10.55493/5005.v15i2.5417
ISSN(P): 2304-1455/ ISSN(E): 2224-4433
How to cite: Ho, T. A., Nguyen, V. K., Bui, V. H., & Nguyen, C. N. (2025). Soil EC index – based prediction of rice growing and yield in the Mekong Delta. *Asian Journal of Agriculture and Rural Development, 15*(2), 281–290.

1. INTRODUCTION
Integrating soil EC with vegetation indices such as the Normalized Difference Vegetation Index (NDVI) and the Normalized Difference Red Edge (NDRE) is a promising approach in precision agriculture, particularly for rice cultivation in the Mekong Delta. Soil EC reflects properties such as moisture, salinity, and texture, which significantly affect rice growth and yield (Ezrin, Amin, Anuar, & Aimrun, 2010), especially in saline-affected regions like the Mekong Delta (Kaveney et al., 2023). NDVI quantifies crop greenness and health, while NDRE detects chlorophyll variations in dense vegetation, overcoming NDVI saturation (Naguib & Daliman, 2022).

The Mekong Delta, Vietnam's primary rice-producing region, faces challenges from salinity intrusion and seasonal flooding, making soil EC a critical tool for assessing soil conditions (Minh et al., 2022). Salinity levels, often exacerbated by climate change and upstream damming, directly impact rice yields, necessitating precise monitoring and management strategies (Kantoush, Binh, Sumi, & La, 2017). Apparent soil EC, measured via electromagnetic induction

and machine learning, maps spatial soil variability in paddy fields (Fletcher, 2022). Temporal soil EC changes reveal soil texture and moisture shifts, influencing water availability and root growth in flooded paddy fields (Ezrin et al., 2010; Fletcher, 2022).

Soil EC impacts rice yield directly and indirectly. In rice fields, high soil EC from salinity caused 26.81% yield loss, as observed in saline-affected regions (Litardo, Bendezú, Zenteno, Pérez-Almeida, & Moran, 2022). In the Mekong Delta, salinity intrusion during the dry season increases soil EC, reducing rice yields in coastal provinces like Tra Vinh and Soc Trang (Hoa, 2023). Moderate soil EC in well-irrigated fields, however, boosts yields by optimizing nutrient availability, aiding site-specific management (Litardo et al., 2022). Proximal soil EC mapping, combined with evapotranspiration data, identifies water-limited yield gaps, supporting sustainable irrigation in the Delta (Nocco et al., 2019).

Soil EC monitoring in the Mekong Delta helps farmers identify saline zones and adjust planting schedules or select salt-tolerant rice varieties. For instance, combining soil EC data with NDVI and NDRE from Unmanned Aerial Vehicle (UAV) imagery allows real-time assessment of rice health during critical growth stages, such as tillering and flowering (Zhang et al., 2025). This approach supports precision agriculture by optimizing water and fertilizer use, reducing losses from salinity stress (Xing & Wang, 2024).

Long Short-Term Memory (LSTM) models enhance yield predictions by capturing temporal dynamics in rice fields. LSTM models integrating satellite imagery, weather, and soil data provide accurate forecasts for rice production (Prakash et al., 2025). A (Convolutional Neural Network) CNN-attention-LSTM model fusing NDVI, NDRE, and meteorological data improves field-scale predictions, adaptable to the Delta's variable climate (Zhou et al., 2023).

In conclusion, soil EC and vegetation indices (NDVI, NDRE) reveal soil-rice yield relationships in the Mekong Delta. High EC from salinity reduces yields, while optimal soil EC enhances productivity (Litardo et al., 2022; Naguib & Daliman, 2022). LSTM in yield prediction supports precision agriculture. This study applies EC and NDVI to assess rice growth in the Mekong Delta, using LSTM to predict yields from soil EC data. Separate experiments were conducted: in Can Tho, where soils are non-saline, soil EC and NDVI data were collected at tillering and flowering stages to monitor rice growth; in Can Tho, Hau Giang, Dong Thap, and Soc Trang, where soils in Soc Trang are saline-affected, soil EC and yield data were collected. These findings optimize farming practices by guiding irrigation, fertilization, and variety selection, enhancing resilience in saline-affected regions.

2. MATERIALS AND METHODS

2.1. Materials

The study was conducted across five regions as follows: Region 1 – (Th_Lai) located at coordinates 10.024103, 105.579156 with an area of 14,000 m² in Thoi Lai District, Can Tho City; Region 2 – (Ch_Th) located at coordinates 9.956722, 105.561388 with an area of 11,000 m² in Chau Thanh District, Hau Giang Province; Region 3 – (C_Lanh) located at coordinates 10.573382, 105.674949 with an area of 8,000 m² in Cao Lanh District, Dong Thap Province; Region 4 – (L_Phu) located at coordinates 9.716630, 105.937126 with an area of 11,000 m² in Long Phu District; and Region 5 – (Tr_De) located at coordinates 9.512352, 106.147022 with an area of 7,500 m² in Tran De District, Soc Trang Province, Vietnam (Figure 1).

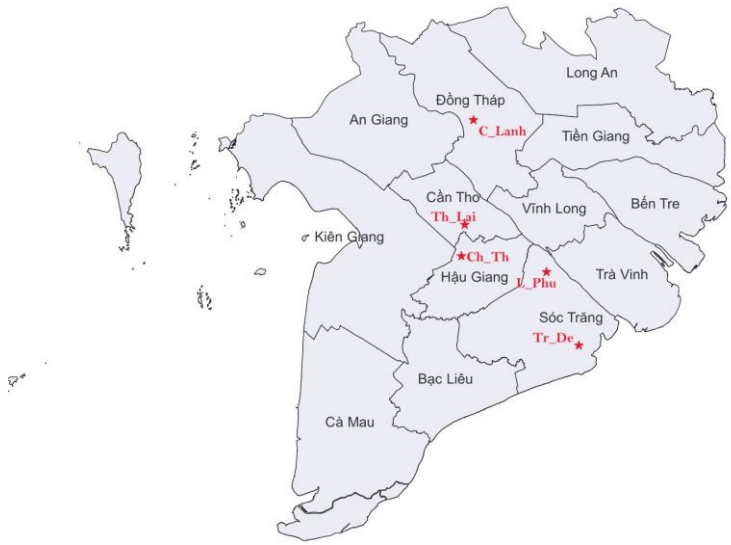

Figure 1. Study area for soil EC and yield data collection.

EC data was collected using the Wenner electrode method with electrode spacings of 10 cm (EC 10) and 30 cm (EC 30), as applied in previous experiments (Ho, Bui, Nguyen, Nguyen, & Nguyen, 2024; Ho, Bui, Nguyen, Nguyen, & Nguyen, 2024). Additionally, soil EC was measured using the Hanna HI98331 soil EC meter, with a measurement range of 0–4 mS/cm, to collect data from the surface soil layer within the device's depth limit of approximately 5 cm. Soil EC was recorded at the beginning of the season and during various rice growth stages, specifically when water was drained from the fields.

In addition to data collected at the start of the season, soil EC data was continuously gathered at different rice growth stages. A Sentera Double 4K camera, mounted on a DJI Phantom 4 RTK UAV (Figure 2), was used to capture RGB color images and spectral images (including NDVI and NDRE images). The UAV-collected NDVI and NDRE images were processed and stitched using Agisoft Metashape software, and the indices were subsequently calculated using QGIS software.

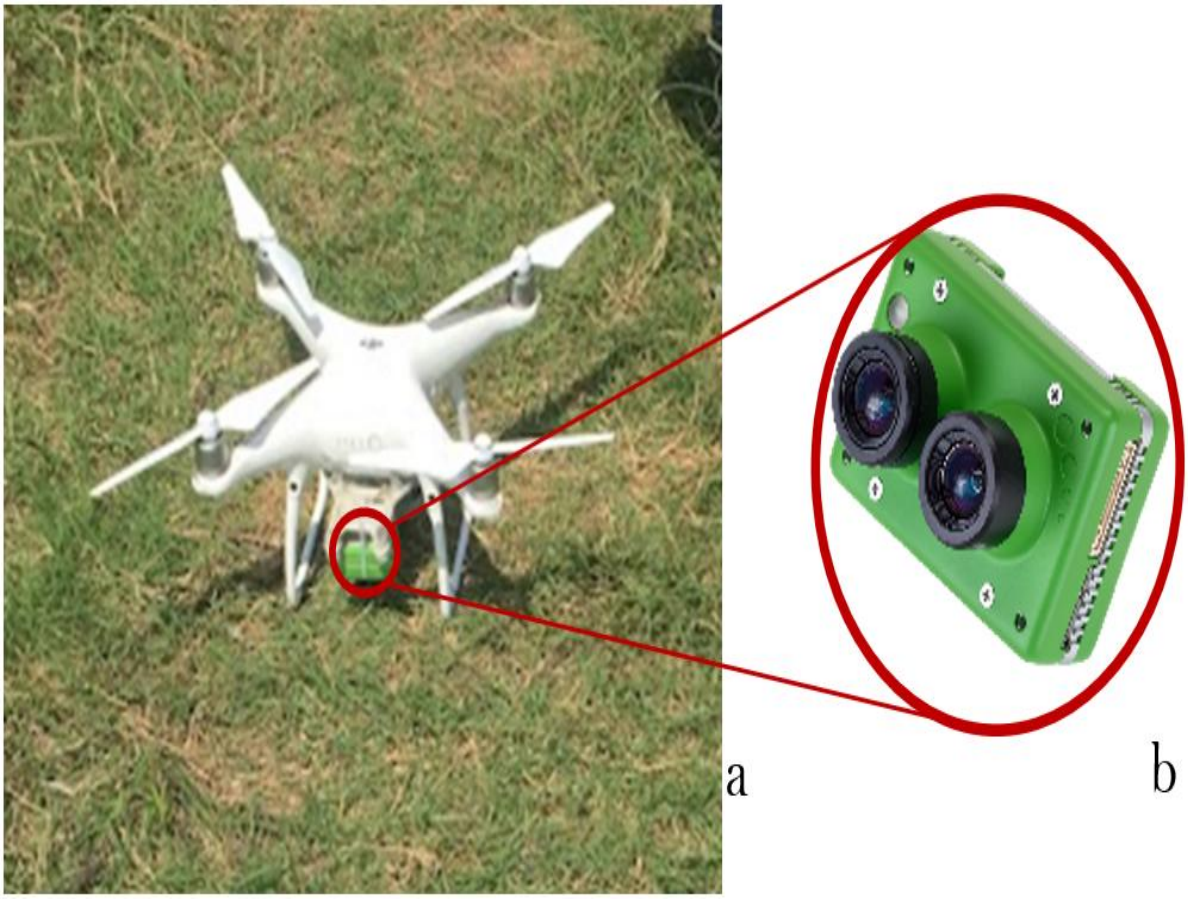

Figure 2. UAV and camera – a) DJI Phantom 4 RTK UAV (Source: Authors) – b) Sentera Double 4K camera.
Source: Senterra sensors, https://senterasensors.com/hardware/sensors/double-4k/.

The NDVI index is calculated using formula (1), with the RED and NIR coefficients determined by formulas (2) and (3), provided by the manufacturer Sentera according to the device's attached documentation.

$$NDVI = (NIR - RED)/(NIR + RED) \quad (1)$$

Where:

$$RED = -0.966 * ChNir + 1.000 * ChRed \quad (2)$$

$$NIR = 4.35 * ChNir - 0.286 * ChRed \quad (3)$$

The NDVI index is calculated using formula (4), with the REDEDGE and NIR coefficients determined by formulas (5) and (6).

$$NDRE = (NIR - REDEDGE)/(NIR + REDEDGE) \quad (4)$$

Where:

$$REDEDGE = -0.956 * ChNir + 1.000 * ChRed \quad (5)$$

$$NIR = 2.426 * ChNir - 0.341 * ChRed \quad (6)$$

Here, $ChNir, ChRed$ the values represent the infrared and red channel indices in the images obtained from the unmanned aerial vehicle..

2.2. Data Collection

2.2.1. Collection of Soil EC, NDVI and NDRE

Depending on the rice variety, cultivation duration, and different farming techniques, the timing of data sampling was adjusted to suit specific conditions. In C_Lanh, during the cultivation process, water was drained at 32 and 49 days after sowing (DAS). At other times, the water level in the field remained stable, preventing soil EC sampling. In Th_Lai, water drainage was carried out at the beginning of the season, and at 39 and 49 DAS *(*Figure 3*)*.

Figure 3. Soil EC collection – a) At the beginning of the season – b) At 49 DAS.

Image data from the UAV was collected at 39, 49, 60, and 72 DAS. The image data includes RGB images captured by the camera pre-installed on the UAV, as well as multispectral image data consisting of NDVI (Figure 4-a) and NDRE images. Fixed points were established to precisely determine the locations of points in the images (Figure 4-b,c) and in the field during the data collection process. The soil EC, NDVI, and NDRE indices were calculated as the average of 6 points in each horizontal row to serve as a basis for comparison. The NDVI and NDRE values were collected using a cluster sampling method in QGIS software (via the Zonal Statistics extension) for each data point in the images.

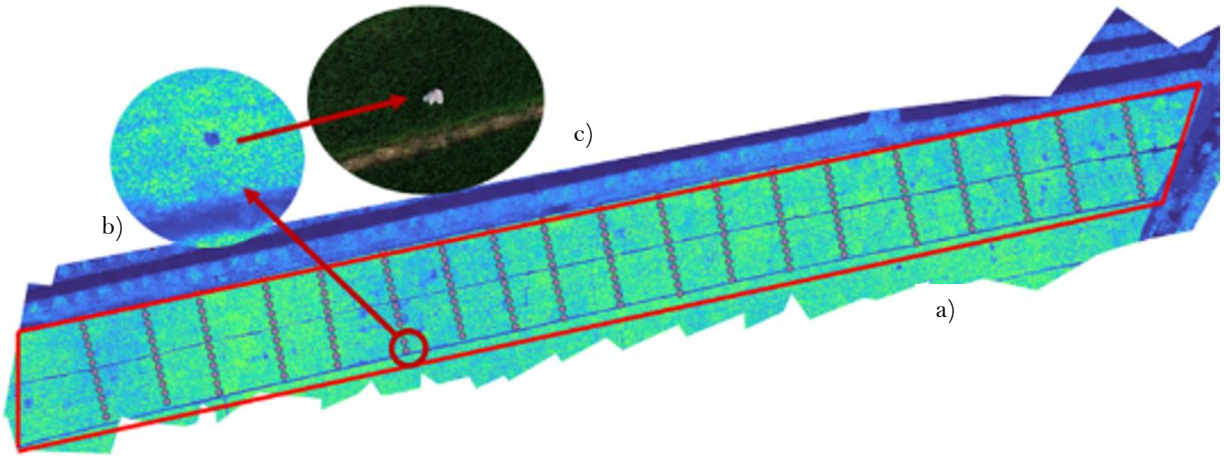

Figure 4. Method for determining positioning points – a) NDVI image at 39 DAS – b) Positioning points in NDVI image – c) Positioning points in RGB image

2.2.2. Soil EC and Yield Collection

The study was conducted at five locations, including Th_Lai, Ch_Th, Ch_Th, L_Phu, and Tr_De, to evaluate rice yield and soil EC at the beginning of the season. Data was collected during the main season of 2025, from October 2024 to February 2025, a period less affected by weather. At each location, 30 positions were randomly selected for surveying.

Rice yield was directly measured at each position's harvested 50 x 50 cm area, then standardized to tons/ha for comparison. Soil EC samples were collected in the morning (from 6 a.m. to 9 a.m.) to ensure consistency in environmental conditions. The data were then analyzed using descriptive statistical methods with Excel software to calculate median values, minimum, maximum, and variation range. Box plots were used to visualize the distribution of yield and EC at each location.

2.3. LSTM Application for Predicting Rice Yield Based on Soil EC

LSTM is a special type of Recurrent Neural Network (RNN) designed to effectively handle long sequence data by addressing the vanishing gradient problem commonly encountered in traditional networks (Chollet, 2021; Patil, 2022). This network is designed to overcome this issue by using a cell state and gates to regulate the flow of information. An

LSTM unit has three main gates: the Forget Gate, the Input Gate, and the Output Gate, along with a cell state to store long-term information *(*Figure 5*)*.

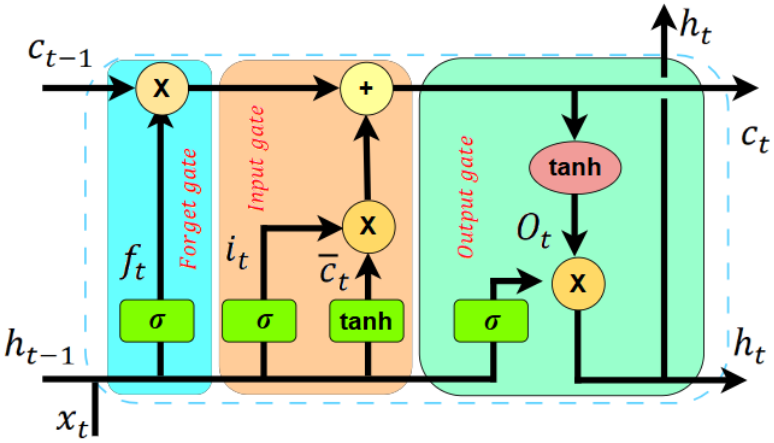

Figure 5. The cell state of the $t-cell$ in the LSTM model.

Where: c_t is the cell state, $h_t$is the hidden state, $x_t$is the input with the soil EC value at the t^{th} state of the model. $c_{t-1}, h_{t-1}$is the output of the previous layer, initially initialized and typically set to 0 for the initial state.

Forget Gate: Determines which information from the previous cell state will be forgotten.

$$f_t = \sigma\left(W_t.[h_{t-1}, x_t] + b_f\right) \quad (7)$$

f_t The forget gate value at time t (in the range [0, 1]).

σ The sigmoid function.

W_t The weight matrix of the forget gate.

h_{t-1} The hidden state from the previous time step.

x_t The input at time t.

b_f The bias of the forget gate.

Input Gate: Determines which information from the current input will be updated into the cell state.

$$i_t = \sigma(W_i.[h_{t-1}, x_t] + b_i) \quad (8)$$

i_t The input gate value at time t.

W_i The weight matrix of the input gate.

b_i The bias of the input gate.

Candidate Cell State:

$$\tilde{c}_t = tanh(W_C.[h_{t-1}, x_t] + b_C) \quad (9)$$

$\tilde{c}_t$ The candidate cell state.

tanh The hyperbolic tangent function.

W_C The weight matrix for estimating the cell state.

b_C The corresponding bias.

Cell State Update: Combines old and new information to update the cell state.

$$c_t = f_t.c_{t-1} + i_t.\tilde{c}_t \quad (10)$$

c_t The cell state at time t.

$\tilde{c}_t$ The cell state from the previous time step.

Output Gate: Determines the output of the LSTM unit based on the current cell state.

$$o_t = \sigma(W_o.[h_{t-1}, x_t] + b_o) \quad (11)$$

o_t The output gate value at time t.

W_o The weight matrix of the output gate.

b_o The bias of the output gate.

Hidden State:

$$h_t = o_t.tanh(c_t) \quad (12)$$

h_tThe hidden state at time t, which is also the output of the LSTM unit.

The LSTM model was implemented using Python (version 3.9) with the TensorFlow library (version 2.10). The model architecture comprised one LSTM layer with 100 units, followed by a Dense output layer, totaling 41,701 trainable parameters. Input features were normalized to a 0-1 scale using min-max scaling. The model was trained for 290 epochs with a batch size of 10, employing the ReLU activation function and the Adam optimizer (learning rate = 0.001). Performance was evaluated using Root Mean Square Error (RMSE), Mean Absolute Error (MAE), and the coefficient of determination (R^2) on 30% of the test data.

3. RESULTS AND DISCUSSION

3.1. Results for soil EC, NDVI, and NDRE

The soil EC 10 value (mS/cm) reached its highest level of approximately 0.52 during land preparation and sowing stages. Subsequently, the soil EC value gradually decreased to 0.38 by the 49-day stage. Since the period after 49 days corresponds to the flowering and grain-filling stages of rice, soil EC measurements could not be conducted during this phase. The continuous decline in soil EC from sowing to around 49 days suggests that changes in soil EC over time may be related to root system development or other factors affecting soil EC during rice growth *(*Figure 6*)*.

The initial NDVI value increased to a peak of about 0.77 at 39 DAS. The NDVI value continued to rise more slowly, reaching its maximum of 0.88 at 49 DAS. Thereafter, it decreased to 0.84 at 60 DAS and further dropped to 0.67 by 72 DAS. The highest NDVI at the mid-stage (49 DAS) indicates that this is the period of the most vigorous rice growth, with the densest leaf and canopy coverage, as reflected by the plant's light absorption and reflection capabilities.

Soil EC values were measured using the Hanna HI98331 device at a depth of approximately 5 cm. At the beginning of the season (6 DAS), the recorded value was 0.76 mS/cm. By day 32, the value increased to 0.86 mS/cm, the highest recorded across all stages. Subsequently, by day 48, it slightly decreased to 0.84 mS/cm. This variation suggests that surface soil EC tends to rise rapidly in the early stages before slightly declining as the rice matures, possibly due to changes in water and ion content in the soil *(*Figure 7*)*.

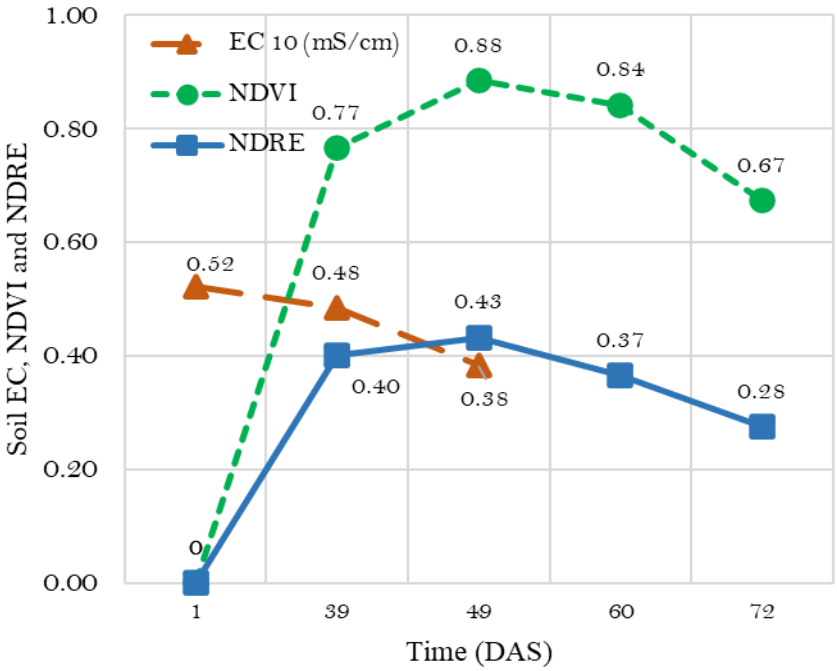

Figure 6. Variations of soil EC, NDVI and NDRE by DAS.

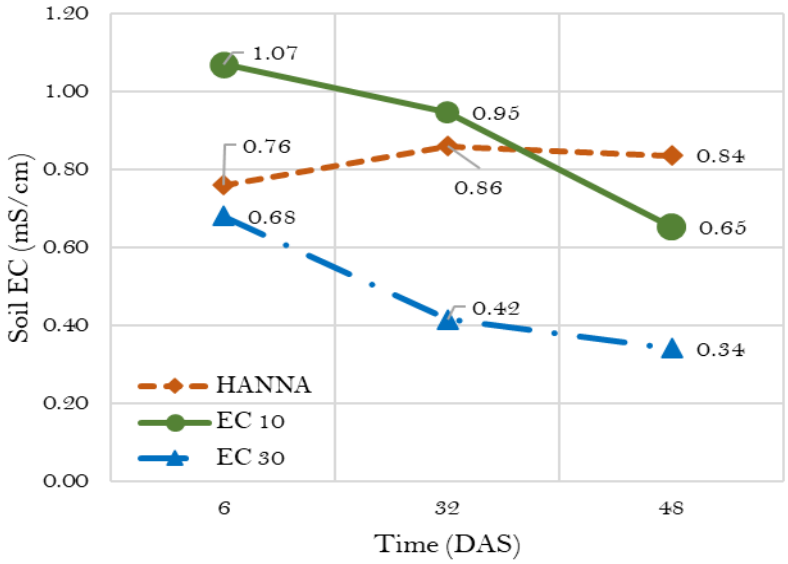

Figure 7. Soil EC fluctuations over DAS.

Soil EC measurements at a 10 cm depth using the Wenner method showed a soil EC 10 value of 1.07 mS/cm on 6 DAS. By 32 DAS, this value decreased to 0.95 mS/cm, and further dropped to 0.65 mS/cm by 48 DAS. This indicates that at a 10 cm depth, soil EC gradually decreases over time, possibly due to nutrient and water uptake by the roots, altering the soil EC of the surface soil layer.

At a depth of 30 cm, EC measurements using the Wenner method recorded a value of 0.68 mS/cm on 6 DAS. This value sharply declined to 0.42 mS/cm by 32 DAS and continued to decrease to 0.34 mS/cm by 48 DAS. At this 30 cm depth, soil EC shows a clear and consistent decline over time, potentially due to the depletion of water and ions in deeper soil layers during plant development or drainage from upper soil layers.

3.2. Result Correlation Analysis

This study focuses on evaluating the relationship between soil electrical conductivity (EC) and rice growth through the NDVI and NDRE indices. Soil EC was measured using the Wenner method at two time points: at the beginning of the season (EC 1, before sowing) and at 49 days after sowing (DAS) (EC 49). The NDVI and NDRE indices were collected using a multispectral camera at the following stages: 39 DAS (NDVI 39, NDRE 39), 49 DAS (NDVI 49, NDRE 49), 60 DAS (NDVI 60, NDRE 60), and 72 DAS (NDVI 72, NDRE 72). The correlation matrix below presents the correlation coefficients (r) between these parameters, with * and ** indicating statistical significance levels ($p < 0.05$ and $p < 0.01$, respectively), and "ns" denoting no statistical significance (Figure 8).

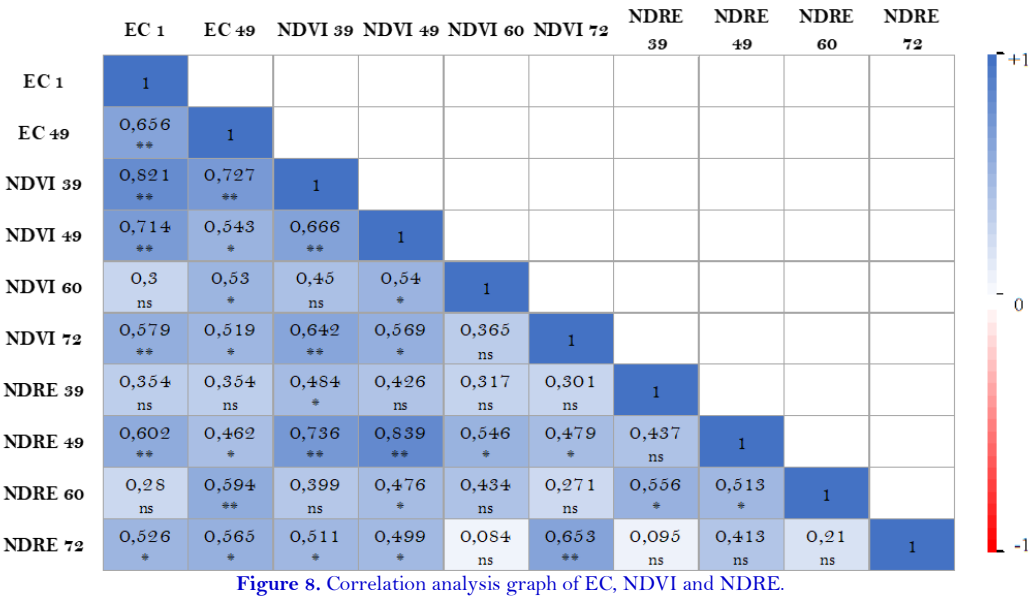

Figure 8. Correlation analysis graph of EC, NDVI and NDRE.

The correlation coefficient between EC 1 and EC 49 is 0.656 (statistically significant **). This suggests that at locations where soil EC is high at the beginning of the season, it tends to remain high after 49 DAS. Initial EC (EC 1) has a strong influence on NDVI 39 ($r = 0.821$) and NDVI 49 ($r = 0.714$), but its influence diminishes at NDVI 60 ($r = 0.579$) and becomes statistically insignificant at NDVI 72 ($r = 0.354$). This indicates that initial soil conditions significantly impact biomass in the early growth stages, but their effect weakens in later stages.

Soil EC at 49 DAS (EC 49) has a moderate influence on NDVI 49 ($r = 0.543$), NDVI 60 ($r = 0.53$), NDRE 49 ($r = 0.462$), NDRE 60 ($r = 0.594$), and NDRE 72 ($r = 0.565$). This shows that EC 49 has a certain impact on plant health, particularly from 49 DAS onward. However, measuring EC data during this period is more challenging due to the increased height of the rice plants.

3.3. Results of Soil EC and Yield Collection

The study results reveal significant variations in rice yield across the surveyed locations (Table 1). L_Phu recorded the highest yield, with an average of 0.98 tons/ha and a wide variation range from 0.89 to 1.25 tons/ha. This indicates that L_Phu has the greatest potential for rice production among the surveyed sites. In contrast, Tr_De exhibited the lowest yield, averaging only 0.36 tons/ha with a narrow variation range from 0.26 to 0.46 tons/ha. This result reflects not only the low yield in Tr_De but also suggests that this area faces significant challenges in rice production, such as more severe saltwater intrusion.

Table 1. Soil EC and rice yield at research locations.

Region	Soil EC max (mS/cm)	Soil EC average (mS/cm)	Soil EC min (mS/cm)	Yield max (Tons/Ha)	Yield average (Tons/Ha)	Yield min (Tons/Ha)
Th_Lai	0.66	0.52	0.40	6.9	6.1	5.5
C_Lanh	1.23	1.07	1.00	10.1	9.0	8.3
Ch_Th	0.96	0.86	0.76	9.0	8.1	6.6
L_Phu	1.56	1.41	1.29	12.5	9.8	8.9
Tr_Đe	2.26	2.11	2.02	4.6	3.6	2.6

At C_Lanh and Ch_Th, the average rice yields were 9.0 tons/ha and 8.1 tons/ha, respectively. The yield variation ranges were from 8.3 to 10.1 tons/ha in C_Lanh and from 6.6 to 9.0 tons/ha in Ch_Th. This indicates that the yields in C_Lanh and Ch_Th are relatively consistent with each other. Meanwhile, Th_Lai exhibited a lower yield compared to C_Lanh and Ch_Th, with an average of 0.61 tons/ha and a narrower variation range, from 5.5 to 6.9 tons/ha (Figure 9).

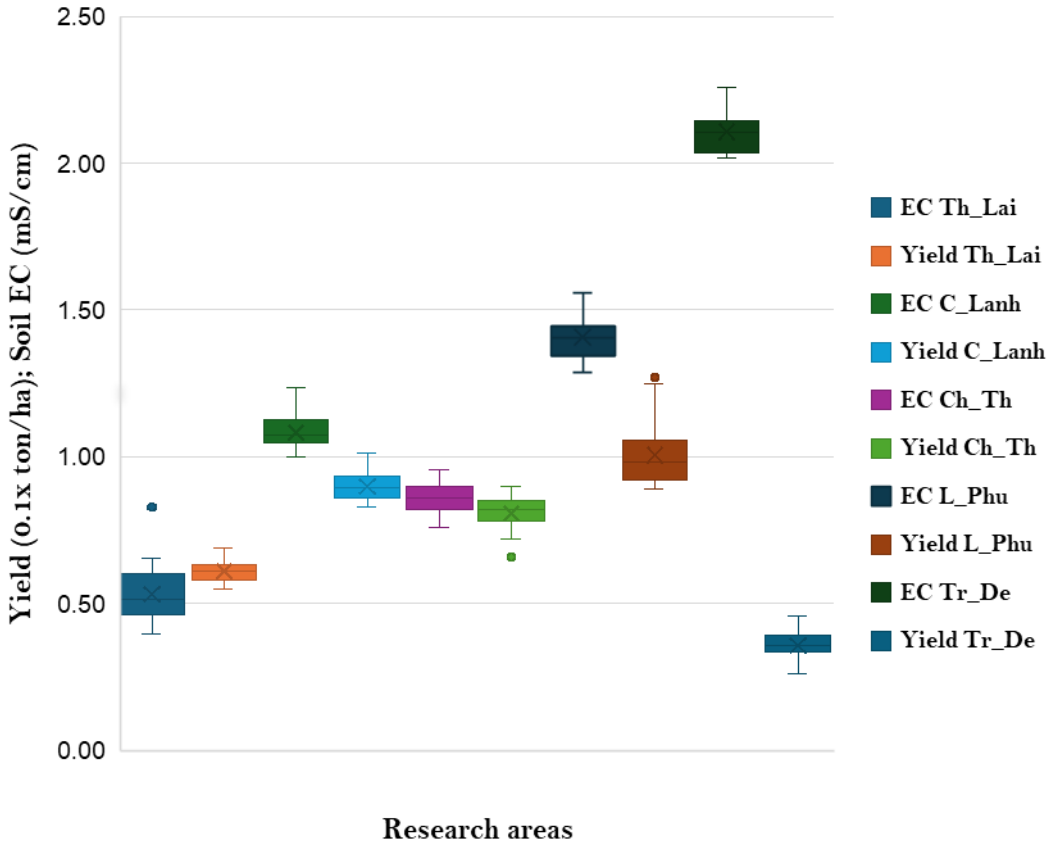

Figure 9. Graph of soil EC and rice yield.

The initial soil EC at the beginning of the season also showed significant differences across the surveyed locations. Tr_De recorded the highest soil EC, with an average of 2.11 mS/cm and a variation range from 2.02 to 2.26 mS/cm. This EC level indicates that salinity in Tr_De is a serious issue, likely having a substantial impact on rice yield in this area. L_Phu had the second-highest EC, with an average of 1.41 mS/cm and a variation range from 1.29 to 1.56 mS/cm, although its salinity is relatively high compared to areas like Ch_Th and C_Lanh.

C_Lanh and Ch_Th exhibited moderate soil EC, with median values of 1.07 mS/cm and 0.86 mS/cm, respectively. The soil EC variation ranges were from 1.00 to 1.23 mS/cm in C_Lanh and from 0.76 to 0.96 mS/cm in Ch_Th, indicating moderate soil EC levels with minimal fluctuation. Meanwhile, Th_Lai had the lowest soil EC, with a median of 0.52 mS/cm and a variation range from 0.40 to 0.66 mS/cm. This EC level suggests that salinity is not a significant issue in Th_Lai; however, the yield in this area is notably lower compared to C_Lanh and Ch_Th.

The study results reveal an inverse correlation between soil EC and rice yield in certain areas. In Tr_De, the highest EC (average 2.11 mS/cm) corresponded to the lowest yield (median 3.6 tons/ha), indicating that salinity is a primary factor limiting rice yield in this region. Conversely, L_Phu, with the second-highest EC (median 1.41 mS/cm), achieved the highest yield (median 9.8 tons/ha). This suggests that in L_Phu, adaptive measures such as the use of salt-tolerant rice varieties or effective water management may have been successfully implemented.

On the other hand, in an area with minimal salinity like Th_Lai, which has the lowest soil EC (average 0.52 mS/cm), the yield was relatively low (average 6.1 tons/ha). As soil EC increases, such as in C_Lanh and Ch_Th with moderate soil EC levels (1.07 mS/cm and 0.86 mS/cm), the corresponding yields were higher (averages of 9.0 tons/ha and 8.1 tons/ha, respectively), aligning with the expectation that moderate soil EC levels may contribute to increased yields in these areas.

3.4. Results of LSTM Application for Predicting Rice Yield Based on Soil EC

The research results when using the LSTM model to predict rice yield based on soil EC indices at the beginning of the season, with a total of 150 datasets collected from Th_Lai, Ch_Th, Ch_Th, L_Phu, and Tr_De regions. The LSTM model was designed with one LSTM layer consisting of 100 units and one Dense output layer, with a total of 41,701 trainable parameters. The model was trained for 270 epochs with a batch size of 10, using the ReLU activation function and optimized with Adam.

For the model using the tanh activation function, the R^2 value ranged from 0.68 to 0.71 (Table 2), with the highest value at 260 epochs (0.71) and a slight decrease at 280 epochs (0.69). This indicates that the tanh model explains approximately 68-71% of the data variance. For the model using the ReLU activation function, the R^2 value ranged from 0.83 to 0.85, with the highest value at 270 epochs (0.85) and a slight decrease at 280 epochs (0.83). This shows that the ReLU model explains approximately 83-85% of the data variance.

Table 2. Performance of different activation functions.

Epochs	tanh			ReLU		
	R^2	MAE	RMSE	R^2	MAE	RMSE
250	0.68	0.09	0.13	0.83	0.06	0.09
260	0.71	0.09	0.13	0.84	0.06	0.09
270	0.70	0.09	0.13	0.85	0.06	0.09
280	0.69	0.09	0.13	0.83	0.06	0.1

Regarding the performance of the model using ReLU as the activation function: The test set loss value was 0.0083, and the RMSE was 0.09, indicating a relatively low average error between predicted and actual values. The MAE value of 0.06 reflects a low average absolute error between predicted and actual values, demonstrating the model's high reliability. The R^2 coefficient of 0.85 indicates that the model explains approximately 85% of the variance in rice yield based on soil EC (Figure 10).

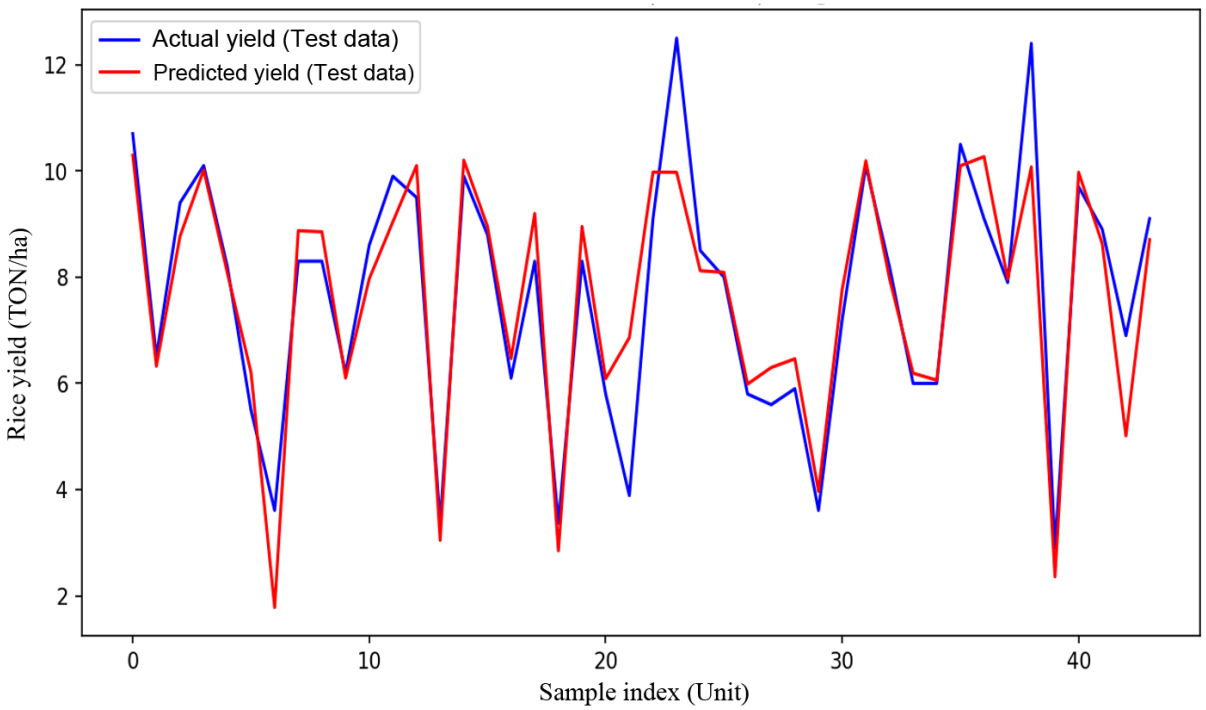

Figure 10. Predicted vs actual rice yield (Test data) using LSTM.

4. DISCUSSIONS

The strong inverse correlation between soil EC 1 and yield in Tr_De (r = -0.82, inferred from the data) underscores salinity as a limiting factor, while the high yield in L_Phu despite a high soil EC 1 (1.41 mS/cm) suggests successful adaptation strategies, such as salt-tolerant varieties or improved irrigation systems. However, several limitations should be considered. First, the model does not account for external variables such as rainfall, temperature, or pest pressure, which may contribute to the 15% of yield variation not explained (R^2 = 0.849). Second, the study was conducted during a period of low salinity (October 2024 to January 2025), potentially underestimating soil EC impact during the peak saltwater intrusion season (February to April). Third, the generalizability of the LSTM model to other rice-growing regions with different soil types or climates remains untested. Therefore, future studies should integrate meteorological data, crop variety-specific responses, and seasonal soil EC measurements to enhance prediction accuracy and broaden applicability.

5. CONCLUSIONS

Soil EC 1 can be used to predict the growth potential of rice in early stages (39 and 49 DAS). If soil EC 1 is excessively high, soil improvement measures should be applied before sowing. Soil EC at 49 DAS affects plant health (NDRE) in later stages, necessitating monitoring and management of soil conditions at 49 DAS to ensure optimal rice development during the flowering and grain-filling stages (60-72 DAS).

With an R^2 value of 0.8492, the results demonstrate that soil EC indices at the beginning of the season can be effectively used to predict rice yield through the LSTM model. This aligns with the fact that soil EC reflects factors such as salinity, moisture, and nutrient content, all of which directly influence rice growth and yield.

However, the R^2 value reaching 85% indicates that approximately 15% of the variation in rice yield remains unexplained by soil EC indices. This could be attributed to other factors such as weather conditions, farming techniques, or additional physiological indicators of the season.

Funding: This study received no specific financial support.
Institutional Review Board Statement: Not applicable.
Transparency: The authors state that the manuscript is honest, truthful, and transparent, that no key aspects of the investigation have been omitted, and that any differences from the study as planned have been clarified. This study followed all writing ethics.
Competing Interests: The authors declare that they have no competing interests.
Authors' Contributions: All authors contributed equally to the conception and design of the study. All authors have read and agreed to the published version of the manuscript.

REFERENCES

Chollet, F. (2021). *Deep learning with Python*. Shelter Island, NY: Simon and Schuster.

Ezrin, M., Amin, M., Anuar, A., & Aimrun, W. (2010). Relationship between rice yield and apparent electrical conductivity of paddy soils. *American Journal of Applied Sciences, 7*(1), 63–70.

Fletcher, R. S. (2022). Temporal comparisons of apparent electrical conductivity: A case study on clay and loam soils in Mississippi. *Agricultural Sciences, 13*(8), 936–946.

Ho, T.-A., Bui, V.-H., Nguyen, V.-K., Nguyen, D.-T., & Nguyen, C.-N. (2024). Development of a soil electrical conductivity measurement system in paddy fields. *International Journal of Advances in Applied Sciences, 13*(2), 389–400. https://doi.org/10.11591/ijaas.v13.i2.pp389-400

Ho, T. A., Bui, V. H., Nguyen, V. K., Nguyen, V. K., & Nguyen, C. N. (2024). An application of soil electrical conductivity measurement by Wenner method in paddy field. *International Journal of Engineering Trends and Technology, 72*(2), 58–68. https://doi.org/10.14445/22315381/IJETT-V72I2P107

Hoa, L. (2023). The impact of saltwater intrusion on rice cultivation and aquaculture in Ham Tan Commune, Tra Cu District, Tra Vinh Province, Mekong Delta, Vietnam. *European Scientific Journal, 19*, 27-33. https://doi.org/10.19044/esj.2023.v19n22p27

Kantoush, S., Binh, D., Sumi, T., & La, T. (2017). Impact of upstream hydropower dams and climate change on hydrodynamics of Vietnamese Mekong Delta. *Journal of Japan Society of Civil Engineers, Ser. B1 (Hydraulic Engineering), 73*, I_109-I_114. https://doi.org/10.2208/jscejhe.73.I_109

Kaveney, B., Barrett-Lennard, E., Minh, K. C., Duy, M. D., Thi, K. P. N., Kristiansen, P., . . . Condon, J. (2023). Inland dry season saline intrusion in the Vietnamese Mekong River Delta is driving the identification and implementation of alternative crops to rice. *Agricultural systems, 207*, 103632. https://doi.org/10.1016/j.agsy.2023.103632

Litardo, R. C. M., Bendezú, S. J. G., Zenteno, M. D. C., Pérez-Almeida, I. B., & Moran, E. S. H. (2022). Salinity of soil and irrigation water on rice productivity in the canton of San Jacinto de Yaguachi, Ecuador. *Agrociencia*. https://doi.org/10.47163/agrociencia.v56i7.2602

Minh, H. V. T., Lavane, K., Ty, T. V., Downes, N. K., Hong, T. T. K., & Kumar, P. (2022). Evaluation of the impact of drought and saline water intrusion on rice yields in the Mekong delta, Vietnam. *Water, 14*(21), 3499. https://doi.org/10.3390/w14213499

Naguib, N., & Daliman, S. (2022). Analysis of NDVI and NDRE indices using satellite images for crop identification at Kelantan. *IOP Conference Series: Earth and Environmental Science, 1102*, 12054. https://doi.org/10.1088/1755-1315/1102/1/012054

Nocco, M. A., Zipper, S. C., Booth, E. G., Cummings, C. R., Loheide, S. P., & Kucharik, C. J. (2019). Combining evapotranspiration and soil apparent electrical conductivity mapping to identify potential precision irrigation benefits. *Remote Sensing, 11*(21), 2460. https://doi.org/10.3390/rs11212460

Patil, S. S. (2022). Deep learning for predictive analytics in Indian agriculture: A case study of crop yield prediction. *Innovative Research Thoughts, 8*(4). https://doi.org/10.36676/irt.v8.i4.1508

Prakash, A., Kaliaperumal, R., Pazhanivelan, S., Muthumanickam, D., Sivamurugan, A., & Govindasamy, V. (2025). Rice yield predictions using remote sensing and machine learning algorithms: A review. *Plant Science Today*. https://doi.org/10.14719/pst.5976

Xing, Y., & Wang, X. (2024). Precise application of water and fertilizer to crops: Challenges and opportunities. *Frontiers in Plant Science, 15*, 1444560. https://doi.org/10.3389/fpls.2024.1444560

Zhang, D., Qi, H., Guo, X., Sun, H., Min, J., Li, S., . . . Lv, L. (2025). Integration of UAV multispectral remote sensing and random forest for full-growth stage monitoring of wheat dynamics. *Agriculture, 15*(3), 353. https://doi.org/10.3390/agriculture15030353

Zhou, W., Song, C., Liu, C., Fu, Q., An, T., Wang, Y., . . . Wang, Q. (2023). A prediction model of maize field yield based on the fusion of multitemporal and multimodal UAV data: A case study in Northeast China. *Remote Sensing, 15*(14), 3483. https://doi.org/10.3390/rs15143483